Agronomy Research **14**(3), 768–778, 2016

Analysis of rapid temperature changes

M. Hromasová* and M. Linda

Czech University of Life Sciences in Prague, Faculty of Engineering, Department of Electrical Engineering and Automation, Kamycka 129, CZ165 21 Praha – Suchdol, Czech Republic
*Correspondence: hromasova@tf.czu.cz

Abstract. The analysis of rapid temperature changes in the dynamic system is described in the paper. Temperature changes are in range of tens of milliseconds. The sensor we used has a significant influence on the dynamic system. In these cases we need to use thermocouples that have appropriate transfer characteristics and can be manufactured with a low time constant. The time constant directly corresponds with weight and size of the sensor. The quality factor is usually in a range between 0.98 and 0.995. Information about the temperature course is particularly important in the field of dynamic systems, e.g. agricultural machines where the switching components are overloaded by pulse switching of technology systems. For the object analysis we use the thermocouples with diameter 0.012 mm with non-encapsulated finish and 0.12 mm with suppression of interference impact and comparative temperature fluctuation. For the analysis of dynamic temperature changes we conduct a measurement with a load factor change, which is the mean value of power change, expressed as ratio of the pulse duration to the delay between pulses, this way we will affect the measurement conditions. As a solution we use measurement methods for a steady state, an impulse test and a method of local measurement of temperature. Compared to a real principle of a component we do not increase temperature of the environment during experiments. The results of measurement can be applied for design and implementation of switching systems for electronic circuits with signal modulation and power load.

Key words: temperature, thermocouple, measurement, sensor, load factor.

INTRODUCTION

In this part of the project we are going to look into a laboratory experiment, a set-up of laboratory environment, used equipment, and into a measurement of dynamic characteristics of a pulse-loaded object. Reference is made to the direct parameter influence of electronic components with rising temperature. In particular it shows the effect on lifetime of loaded components, which after a number of loads, change their specific parameters, and this subsequently leads to their destruction. In this case, attention is drawn to the passive components (Xu et al., 2015; Contento & Semancik, 2016; Song et al., 2016). Another reason why it is important to know the temperature waveform of electronic components are the noise characteristics, especially for circuits, where a very low voltage levels are processed. The amount of noise is influenced by the temperature of resistors and semi-conductor components. We distinguish between thermal noise, shot noise, flicker noise, crackling noise, and total noise. The thermal noise (white noise) is caused by random motion of free electrons in the crystal lattice of

the substance. Shot noise (Schottky noise) is formed by the passing of a current through the PN junction (Huesgen et al., 2008; Häb et al., 2015; Chen et al., 2015). The flicker noise occurs at the base-emitter junction, it is caused by technological impurities and applied at 0.1–10 Hz. The crackling noise again arises at the base-emitter junction, and is characterized by jumps between discrete noise levels (Milton et al., 1997; Jiao et al., 2015; Mirmanto, 2015).

MATERIALS AND METHODS

The input signal of the pulse-loaded object is created by a pulse generator with a set power, where the load factor z is changed (can be quoted in %) (1) (O'Sullivan & Cotterell, 2001).

$$z = \frac{t_1}{T} = \frac{t_1}{t_1 + t_2} \tag{1}$$

The load factor is defined as a ratio of the pulse duration t_1 to the period $T = t_1 + t_2$, when t_2 is dwell time between pulses. The supplied medium power of periodic pulses to the loaded object is according to (2) (O'Sullivan & Cotterell, 2001), see Fig. 1.

$$\overline{P} = \frac{P_1 t_1}{T} = P_1 z\,, \tag{2}$$

where: P_1 *(W)* constant power delivered at the time $0 < t < t_1$.

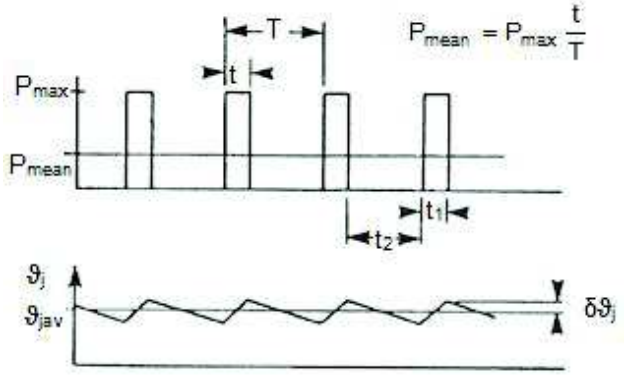

Figure 1. Demonstration of a medium power waveform in time, effect of the load factor (ϑj – an ideal temperature waveform, ϑjav – mean value of an ideal temperature waveform, δϑj – max. temperature deviation on power pulse remission).

The established laboratory environment (see Fig. 2) for measurement of pulsed temperatures waveforms on selected power loaded objects, is comprised of:

- pulse generator, which generates a specified pulse changes of the power;
- loaded/measured object (in our case we chose resistor, which is suitable electronic element for its electrical properties, its behavior was examined by selected methods);

- measuring devices - thermocouple probe, thermoelectric voltage amplifier and a recording device (Sessler & Moayeri, 1990; Huesgen et al., 2008; Chen et al., 2015).

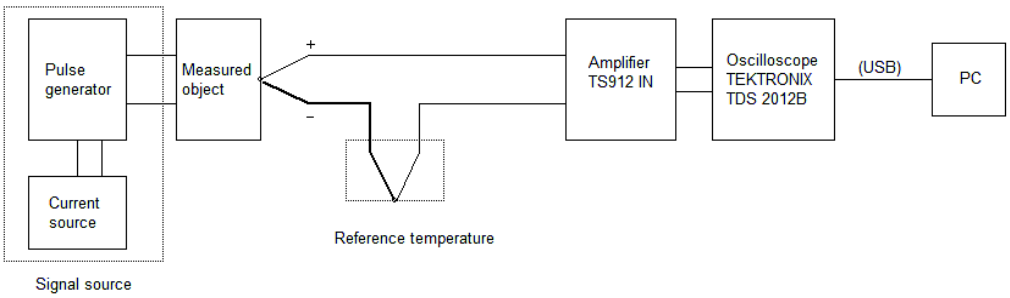

Figure 2. Block diagram of a measuring scheme.

We used a thermocouple with low time constant for measuring the dynamic power pulses, in order to capture the rapid temperature change with sufficient accuracy. The time constant is one of the main parameters of temperature sensors used for measurement of dynamic systems.

For measurement we used a probe 5TC – TT (PFA wire insulation, 914 mm length, wire diameter 0.12 mm). Type K thermocouple with wire diameter of 0.012 mm is designed for spot measurements with high accuracy and low heat transfer. It is suitable for measurement on small objects e.g. SMD resistors, which would not be possible to measure with other type of sensor.

Used measuring methods can be divided into three groups, where the third group complements the previous two, mainly in its functional nature.

The first method 'The measurement of a steady-state' is based on measuring surface temperature of the electric component up until its stabilization, i.e. until the input and output energy into the surroundings is balanced. This method is favorable for the possibility to observe the component's behavior at a permanent load, or up to the critical load, and subsequently concludes how many of such cycles the component is capable to endure without an evident damage, or without changing parameters (CXu et al., 2015; Song et al., 2016).

This method is showing an apparent oscillation when measured with a micro thermocouple, which is only a reaction to the measurement of the power pulses, and this change is detailed in another type of test. We can explain this phenomenon by pulse-loading the resistor layer, which is relatively less heavy than the inner layer of ceramic and coating layer. There's a sharp increase of measured surface temperature when influenced by power, without the component being warmed up, when disconnected from the power there's a sharp temperature drop, because of the heat dissipation through ceramics. This phenomenon is not as evident in the second type of thermocouple, where there is furthermore a heat dissipation through conductors that have 10 times larger diameter.

The second method 'The Pulse Test' is based on examination of the surface temperature waveform as a response to one or more pulses at the input of the system, as in our case. In this method, we can significantly increase the load factor and examine the

dynamics of the component during a critical short-term load. The result of such analysis is not only about the exact dynamics of the response, but also about the maximum transferable power of the component.

The complementary method, which is primarily used to analyze temperature distribution on the electronic component's surface, is called 'The method of measuring local temperature'. In our case, we chose it with regard to selected resistors, where because of dimensions, is convenient to know waveforms of the thermal gradient on the component's surface. This method can be extended to a surface measurement. However, an important prerequisite is an accurate matrix arrangement of sensors, see Fig. 4, which creates a basis for the method, see Fig 3. This method can detect subsurface defects in materials, where disruption of the temperature field leads to a distortion of measured temperature in one or more network nodes (Zhao et al., Yang, 2015; Ya et al., 2016).

Figure 3. Block diagram of the power-loaded resistor.

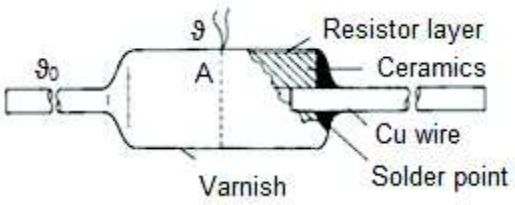

Figure 4. Indication of areas suitable for measuring the resistor's surface temperature.

RESULTS AND DISCUSSION

The Fig. 5 shows the waveform for the first set of parameters, which are listed in column 1 of the Table 1. The temperature waveform during measurement with micro thermocouple reaches an average mean value in a steady-state of 220 °C, and the dispersion of the mean surface temperature of ± 26 °C. Measurement of the temperature dispersion is determined by the type and the time constant of the measuring scheme. Measurement with the second thermocouple version records the reading of stagnation temperature at 121 °C with considerably lower dispersion. This difference is caused by the sensor with higher time constant, and provided that the sensor will transfer heat, as mentioned in the theoretical analysis of the case.

At a temperature of about 150 °C a damage of the resistor's lacquer layer occurred. Measurement was carried out in the laboratory environment with an ambient temperature of 24 °C. These conditions are as close as possible to the work conditions of the analyzed component, where the component is placed inside the device, and is not significantly influenced by ambient conditions, just by the conditions inside the device. However, compared to the real function of the component, the ambient temperature was not increased during the experiment, which significantly impacts the cooling of the resistor.

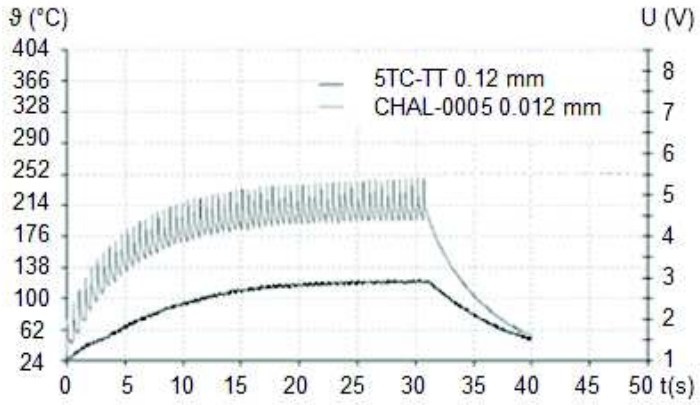

Figure 5. The measured waveform - case a) z = 0.0385.

Table 1. Load factor parameters

Parameters/load factor	0.0385	0.0566	0.0741
Number of cycles n_p (-)	60	60	60
Pulse duration t_s (ms)	20	30	40
No pulse period t_2 (ms)	500	500	500

Fig. 6 shows the temperature waveform when the load factor was changed to a value z = 0.0566, and the mean temperature rises to 260 °C ± 26 °C, and in the second case the temperature rises to 170 °C.

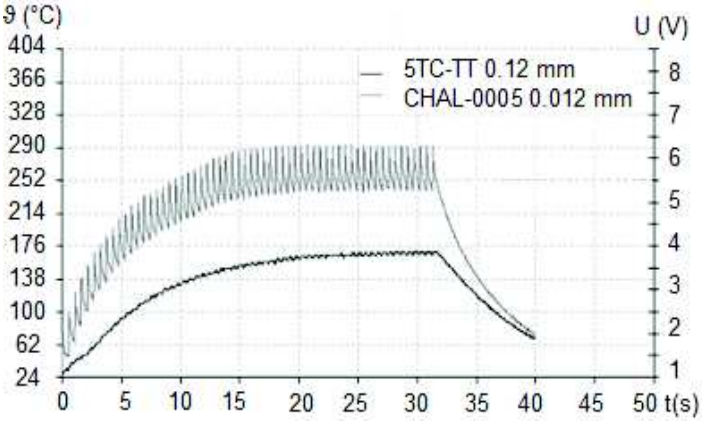

Figure 6. The measured waveform – case b) z = 0.0566.

The dispersion is within the same range for both cases. Overall, it can be concluded, that the measurement is within range of safe operation area, although there is damage to the component's surface layer, it is possible to run it for a certain period of time. The operating state can be considered as a critical operating state without damaging the object. However, in another case we are at the border of a physical lifetime of the object.

Fig. 7 shows the temperature waveform for z = 0.0741, and the mean temperature is 340 °C with ± 38 °C, and for the second case the temperature is 243 °C. In this analysis, the load factor change by 10 ms t_1 does not tally with temperature changes, as in previous cases. The influence is more significant in this very critical state, which damages the component by evaporating the protective layer. After this test, the component is already substantially damaged, and there is no guarantee of its further 100% activity without changing the parameters.

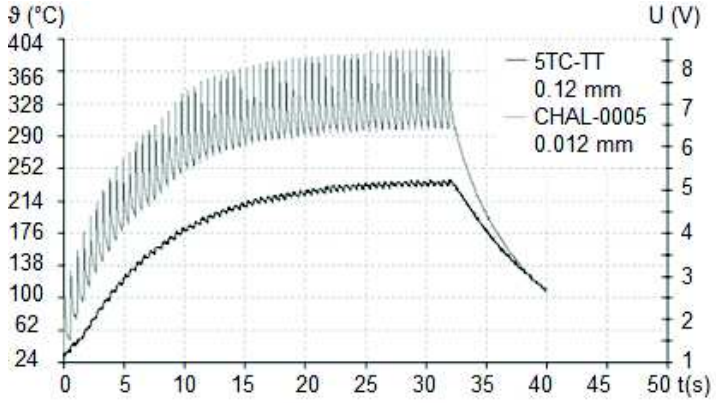

Figure 7. The measured waveform – case c) z = 0.0741.

The analysis indicates that the sensor's measuring part has a clear dependence and impact on quality of object's measured temperature, which significantly influences the use of measuring sensors with regard to measuring possibilities.

From the analysis of the second and the third case, there is a noticeable difference in a steady state of 80 °C for micro thermocouple 0.012 mm, and 73 °C for thermocouple 0.12 mm. At this stage the damage to the components is present, yet without loss of functionality and with no guarantee of maintaining characteristic parameters when an excessive overload leads to a degradation process in the component.

In the case analysis can be noted a decrease of measured surface temperature in time sphere less than 2.5 s. The decrease is caused by heat dissipation through resistor's intakes when the temperature gradient of the component is changing, and influencing significantly the heat transfer through wiring. After a certain period of time the heat dissipation by radiation begins to prevail, and to a certain extent, the heat dissipation through wiring is suppressed. This phenomenon can be observed in all performed measurements, but there is a time shift in measurement of components with higher heat capacity.

Other cases are based on the Pulse test method. The system analysis is examined when five power pulses are on the input. For comparison, two types of load factor changes were chosen when changing the time interval t_2 100 ms and 50 ms.

As anticipated, from the waveforms we can determine the inertia of the system and its order. Inertia manifests itself by the temperature increase even after subsiding of the power pulse.

Fig. 8 and Fig. 9 show first examples of waveforms, where the first represents measurement with a load factor z = 0.167, and the second with z = 0.286. The figures show the influence of the measuring sensor when these rapid power changes of the surface temperature can not be captured by the second sensor.

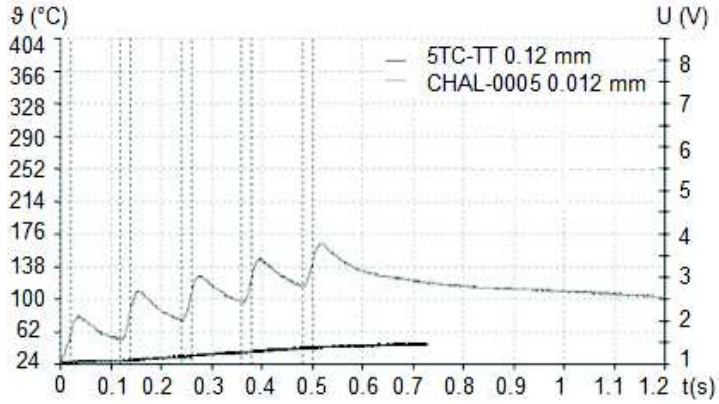

Figure 8. The measured waveform – case a) z = 0.167.

Temperature differences between the pulses can not be linear according to previous measurements. Another dependence, which is determined by inertia of the system, is the temperature increase after the pulse had subsided, this condition can be, to a certain extent, accurately simulated by created model.

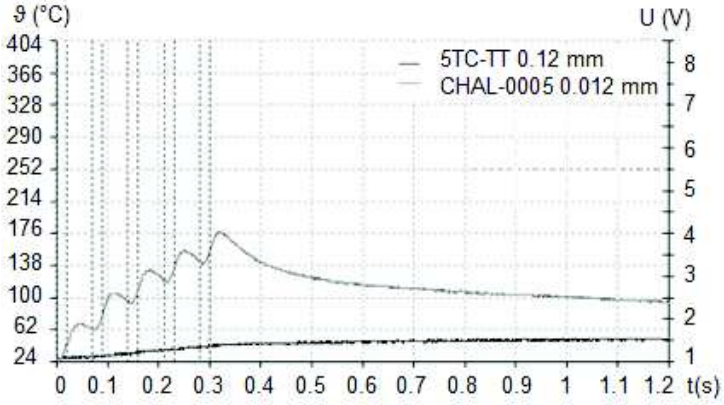

Figure 9. The measured waveform – case b) z = 0.286.

From previous cases, there is an apparent correlation of the component's warming, where the higher load factor leads to a faster warming of the component. In this setting the increase in temperature is less than in setting t_2 = 100 ms.

Another set of waveforms (see Fig. 10 and Fig. 11) represents a change of load factor z = 0.231 to z = 0.375. Maximum temperature of 220 °C was achieved.

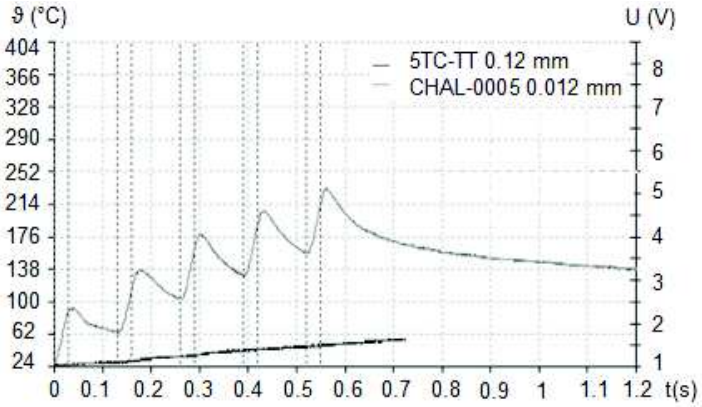

Figure 10. Measured waveform – case a) z = 0.231.

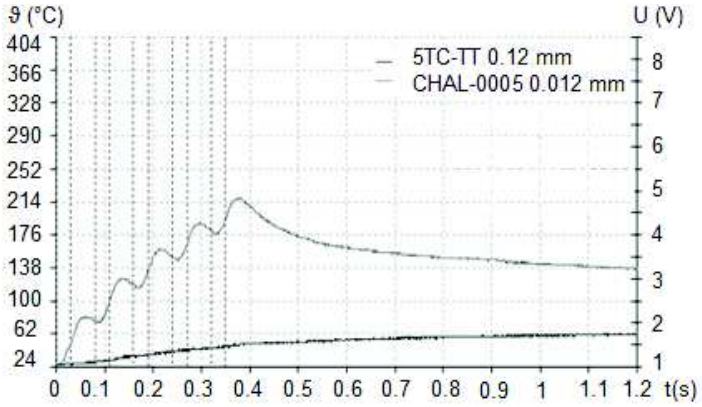

Figure 11. Measured waveform – case b) z = 0.375.

Established results were recorded. The analysis shows a non-linear dependence of achieved temperatures with load factor change. The result is clearly influenced by the heat dissipation through heat emission and wiring, and the temperature gradient is significantly higher when the load factor and maximum temperature are higher. Interdependence of experiments are in Tab. 2a, 2b and 2c.

Table 2 a. Experimental part – results – t_1 = 20 ms; t_2 = 500 ms, n_p = 60; z = 0.03846

Time (s)	5 s	10 s	15 s	20 s	25 s	30 s
resistor 2.2 Ω – 0.5 W						
0.12 mm	64 °C	90 °C	110 °C	115 °C	120 °C	125 °C
0.012 mm	150 °C	184 °C	200 °C	210 °C	216 °C	220 °C
resistor 2.2 Ω – 1 W						
0.12 mm	35 °C	40 °C	50 °C	53 °C	55 °C	56 °C
0.012 mm	37 °C	46 °C	55 °C	57 °C	62 °C	64 °C

Table 2 b. Experimental part – results – t_1 = 30 ms; t_2 = 500 ms, n_p = 60; z = 0.0566

Time (s)	5 s	10 s	15 s	20 s	25 s	30 s
resistor 2.2 Ω – 0.5 W						
0.12 mm	90 °C	135 °C	145 °C	160 °C	165 °C	170 °C
0.012 mm	178 °	231 °C	260 °C	265 °C	270 °C	273 °C
resistor 2.2 Ω – 1W	39 °C	45 °C	58 °C	61 °C	64 °C	75 °C
0.12 mm						
0.012 mm	41 °C	55 °C	62 °C	70 °C	75 °C	79 °C

Table 2 c. Experimental part – results – t_1 = 40 ms; t_2 = 500 ms, n_p = 60; z = 0.0741

Time (s)	5 s	10 s	15 s	20 s	25 s	30 s
resistor 2.2 Ω – 0.5 W						
0.12 mm	125 °C	180 °C	213 °C	220 °C	225 °C	230 °C
0.012 mm	234 °C	295 °C	328 °C	330 °C	340 °C	345 °C
resistor 2.2 Ω – 1 W	41 °C	58 °C	63 °C	70 °C	75 °C	80 °C
0.12 mm						
0.012 mm	43 °C	62 °C	66 °C	82 °C	90 °C	102 °C

Fig. 12 shows a graphical dependence of recorded samples in Tab. 2 a, 2 b and 2 c, and represents dependence and comparison of temperature vs. load factor in time sphere. See picture for evident dependencies of used thermocouples. There is an evident flattening on the other set of pictures, that is caused by this factor.

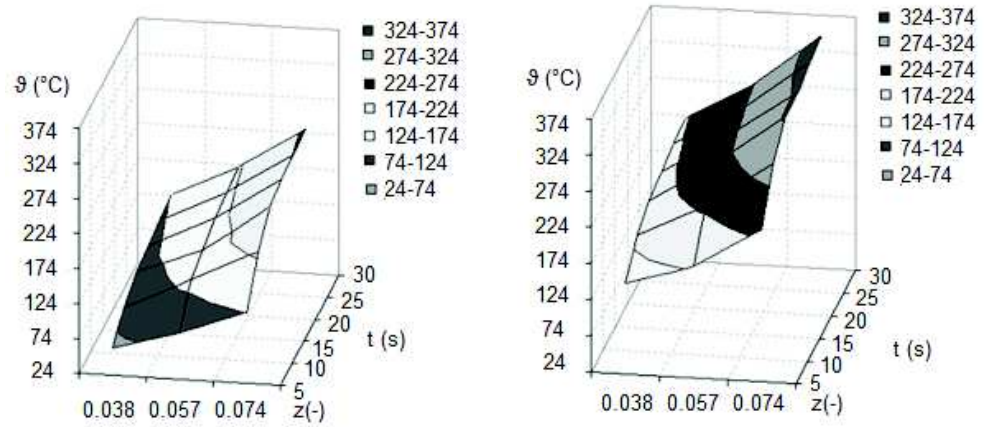

Figure 12. 3D dependency graph of surface temperature vs. load factor, resistor 0.5 W measured with thermocouple 0.12 mm and 0.012 mm.

CONCLUSIONS

- Established workplace for testing temperature sensors, measurement of static and dynamic characteristics, established workplace for testing electrical components;
- models of dynamic properties of objects in rapid time changes, the suitability of using the sensors with different time constant;

- design and development of measuring methods of electrical objects according to the nature of activity, applicability of each method;
- results of surface temperature waveforms on resistors with load factor change, as per measuring methods;
- establishing the effect of load factor change on maximum warming, the evaluation of graphic dependencies between measurements.

The results recommend the contact measurement of temperature. A short term temperature rise can occur during the object analysis, which can not be detected by the sensors and therefore can not flexibly respond to a coming fault that usually manifests itself as a pulse change or as an offset of the system temperature. During the surface/contact measurements we have to take into consideration several factors, such as quality of the surface (polished, oxidized, rough), symmetry of the surface (curved) and a treatment of the surface (varnishing, laminating), the heat dissipation of the sensor, thermal conductivity at the contact, etc.

The analysis of the pulsed temperature change on the electrical object is used with regard to its possible load factor in control systems. Information about the temperature waveform, e.g. on the resistor or the semiconductor component of the power supply or the switch device, when long-term monitored, provides figures that are suitable for establishing the maximum temperature of objects, their dimensioning or diagnostics.

REFERENCES

Contento, N.M. & Semancik, S. 2016. Thermal characteristics of temperature-controlled electrochemical microdevices. *Sensors and Actuators B: Chemical* **225**, 279–287.

Häb, K., Ruddell, B.L. & Middel, A. 2015. Sensor lag correction for mobile urban microclimate measurements. *Urban Climate* 14, 622–635.

Huesgen, T., Woias, P. & Kockmann, N. 2008. Design and fabrication of MEMS thermoelectric generators with high temperature efficiency. *Sensors and Actuators A: Physical* **145–146**(1–2), 423–429.

Chen, S., Li, H., Lu, S., Ni, R. & Dong, J. 2015. Temperature measurement and control of bobbin tool friction stir welding. *The International Journal of Advanced Manufacturing Technology*, 1–10.

Jiao, L., Wang, X., Qian, Y., Liang, Z. & Liu, Z. 2015. Modelling and analysis for the temperature field of the machined surface in the face milling of aluminium alloy. *The International Journal of Advanced Manufacturing Technology* **81**(9–12), 1797–1808.

Milton, N., Pikal, M.J., Roy, M.L. & Nail, S.L. 1997. Evaluation of manometric temperature measurement as a method of monitoring product temperature during lyophilization. *PDA Journal of Pharmaceutical Science and Technology* **51**(1), 7–16.

Mirmanto, M. 2015. Local pressure measurements and heat transfer coefficients of flow boiling in a rectangular microchannel. *Heat and Mass Transfer* **52**(1), 73–83.

O'Sullivan, D. & Cotterell, M. 2001. Temperature measurement in single point turning. *Journal of Materials Processing Technology* **118**(1–3), 301–308.

Sessler, D.I. & Moayeri, A. 1990. Skin-surface warming: heat flux and central temperature. *Anesthesiology* **73**(2), 218–224.

Song, H., Zhan, X., Li, D., Zhou, Y., Yang, B., Zeng, K., Zhong, J., Miao, X. & Tang, J. 2016. Rapid thermal evaporation of Bi2S3 layer for thin film photovoltaics. *Solar Energy Materials and Solar Cells* **146**, 1–7.

Xu, Y., Huang, Y., Wang, X. & Lin, X. 2015. Experimental study on pipeline internal corrosion based on a new kind of electrical resistance sensor. *Sensors and Actuators B: Chemical* **224**, 37–47.

Ya, W., Pathiraj, B. & Liu, S. 2016. 2D modelling of clad geometry and resulting thermal cycles during laser cladding. *Journal of Materials Processing Technology* **230**, 217–232.

Zhao, X., Yang, K., Wang, Y., Chen, Y. & Jiang, H. 2015. Stability and thermoelectric properties of ITON:Pt thin film thermocouples. *Journal of Materials Science: Materials in Electronics*.